

COMMUNICATION

[View Article Online](#)
[View Journal](#) | [View Issue](#)

 Cite this: *Phys. Chem. Chem. Phys.*, 2016, 18, 5095–5098

 Received 1st December 2015,
 Accepted 14th January 2016

DOI: 10.1039/c5cp07400b

www.rsc.org/pccp

The spectroscopic properties of a poly(methyl methacrylate) matrix doped with a coumarin dye, a cyanine dye, and a photochromic spiropyran dye have been investigated. Before UV irradiation of the matrix, excitation of the coumarin dye results in minimal energy transfer to the cyanine dye. The energy transfer is substantially enhanced following UV irradiation of the matrix, which converts the colourless spiropyran isomer to the coloured merocyanine isomer, which then acts as an intermediate bridge by accepting energy from the coumarin dye and then donating energy to the cyanine dye. This demonstration of a switchable energy transfer cascade should help initiate new research directions in molecular photonics.

Many photochromic molecules are characterised by having two distinct isomeric forms, with one being colourless and the other coloured.^{1,2} Because the isomers have different electronic and chemical properties, and can be interconverted using light, together they function as a molecular switch. Possible applications for molecular switches include data storage, molecular motors, biological imaging, and sensors.^{1–6}

The modulation of photonic or photochemical events by molecular switches can be accomplished using Förster resonance energy transfer (FRET), which involves electronic energy being passed between chromophores *via* long-range dipole-dipole coupling. Previous studies have employed the coloured form of a molecular switch as either a FRET donor or acceptor to trigger or quench, respectively, photophysical process in an external molecule or material.^{7–15} In this communication, we describe the use of the coloured form of a molecular switch as a simultaneous FRET donor and acceptor for the first time. As shown in Fig. 1, the FRET cascade scheme utilises the spiropyran (SP)/merocyanine (MC) photochromic system and involves energy transfer from a blue-absorbing coumarin dye (C314) to a near-IR-absorbing cyanine dye (HITC) *via* the

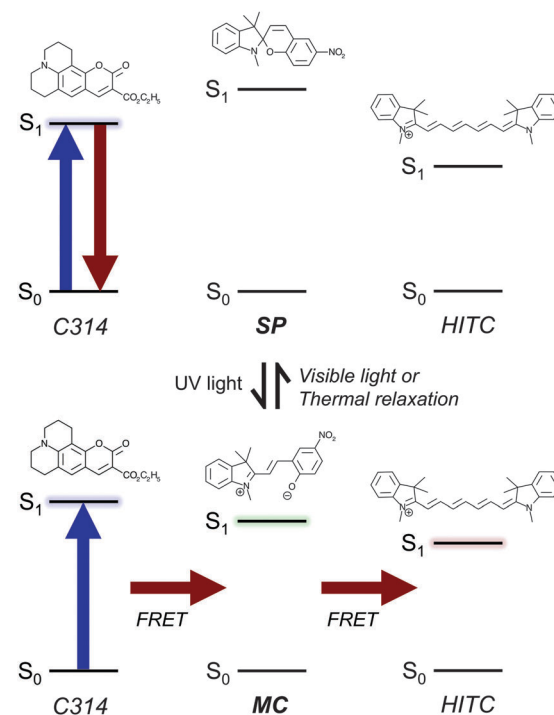


Fig. 1 The photochromic FRET cascade scheme employed in this study: the isomeric state of the SP/MC system either impedes or facilitates C314 to HITC energy transfer.

coloured, ring-opened MC isomer, with this pathway disabled when MC is converted to the colourless, ring-closed SP isomer.

For our experiments we have incorporated the dyes in a poly(methyl methacrylate) (PMMA) polymer matrix. As shown in Fig. 2, the absorption and emission maxima of C314 occur at 435 nm and 470 nm, respectively, whereas for HITC they appear at 755 nm and 780 nm, respectively. Before UV irradiation, the SP/MC sample has an absorption maximum at 345 nm that is due to the SP isomer, which is the lowest energy isomer.^{2,9} Following UV irradiation ($\lambda_{\text{ex}} = 365$ nm) of the matrix, a new

School of Chemistry, The University of Melbourne, Victoria 3010, Australia.

E-mail: vdryza@unimelb.edu.au

† Electronic supplementary information (ESI) available: Experimental procedure and additional results. See DOI: [10.1039/c5cp07400b](https://doi.org/10.1039/c5cp07400b)



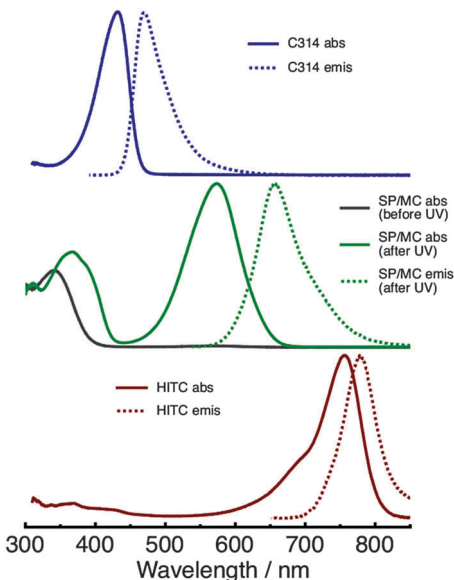


Fig. 2 Normalised absorption and emission spectra of the C314 (top panel), SP/MC before and after UV irradiation (middle panel), and HITC (bottom panel) PMMA samples.

optical absorption band with a maximum at 575 nm appears, which is due to MC.^{2,9} Excitation of MC at 532 nm yields an emission band with a maximum at 655 nm. The UV absorption region is also altered, with the absorption maximum shifting to 370 nm, as MC has an absorption band in this region that overlaps that of SP.^{2,9} These UV-induced spectral changes result from SP \rightarrow MC photoisomerisation, with an estimated conversion of $\sim 60\%$ (see ESI[†]). MC \rightarrow SP isomerisation occurs either through visible irradiation or thermal relaxation.

The efficiency of FRET between donor and acceptor can be related to the Förster distance (R_0), which is the donor–acceptor distance at which the FRET quantum yield (Φ_{FRET}) is 0.50. Using the individual dyes' spectroscopic parameters,^{9,16–18} the C314 + HITC, C314 + MC, and MC + HITC pairs are calculated to have $R_0 = 3.8$ nm, 4.1 nm, and 5.5 nm, respectively (see ESI[†]).

For a mixture of donors and acceptors, Φ_{FRET} is also influenced by the number of acceptors surrounding a donor. Here, we aimed to produce a dye-doped PMMA matrix where the concentrations are such that direct C314 \rightarrow HITC FRET is minimal before UV irradiation (SP/MC predominantly in SP form), with the C314 \rightarrow MC \rightarrow HITC FRET cascade becoming the dominant process following UV irradiation (SP/MC predominantly in MC form). This arrangement allows the state of the SP/MC molecular switch to control the overall amount of C314 to HITC energy transfer.

The C314 + SP/MC + HITC PMMA matrix sample was prepared with a dye concentration ratio of 10 : 50 : 1 (see ESI[†]). The absorption and emission spectra of the sample, before and after UV irradiation, are shown in Fig. 3. Before UV irradiation, the absorption bands of SP, C314, and HITC are clearly evident, and have minimal overlap. Excitation at 435 nm primarily excites C314, producing mainly C314 emission, together with very minor HITC emission. Following UV irradiation, the

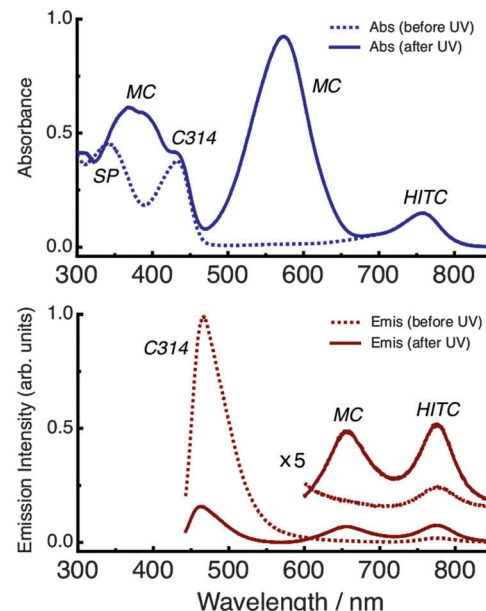


Fig. 3 Absorption (top panel) and emission (bottom panel, $\lambda_{\text{ex}} = 435$ nm) spectra of the C314 + SP/MC + HITC PMMA sample, before and after UV irradiation.

optical absorption band of MC appears, which is located in between the absorption bands of C314 and HITC. Subsequent excitation at 435 nm excites the C314 dye, but now with a $\sim 80\%$ reduction in the C314 emission band's intensity, coupled with the appearance of the optical emission band of MC, indicating C314 \rightarrow MC FRET. Additionally, there is a ~ 4 -fold increase in the HITC emission band's intensity, consistent with MC \rightarrow HITC FRET. Although direct excitation of MC is possible, and C314 \rightarrow MC and MC \rightarrow HITC radiative energy transfers can also occur, they are expected to play a minor role compared to the FRET cascade.

The combined integrated areas of the MC and HITC emission bands after UV irradiation do not reach that of C314 before UV irradiation, most likely because MC and HITC have much lower fluorescence quantum yields (Φ_{R}) than C314: 0.20 and 0.28, compared to 0.83, respectively.^{18,19} In principle, the fluorescence after UV irradiation could be elevated by using an acceptor dye with a high Φ_{R} and having Φ_{FRET} from MC being essentially unity.

The measured spectra are consistent with the UV-generated MC population acting as an intermediate FRET bridge, facilitating C314 \rightarrow MC \rightarrow HITC energy transfer. Furthermore, by alternating between visible and UV irradiation treatments, reversible switching between SP and MC dominant populations is possible, enabling the FRET cascade to be modulated (Fig. 4).

To investigate the mechanism for the FRET cascade further, we measured the fluorescence decay curves of C314 and MC in various PMMA samples where they act as the FRET donor, as shown in Fig. 5. This allows the C314 \rightarrow MC and MC \rightarrow HITC steps within the FRET cascade to be characterised individually. In the samples containing only the donor, we fit the decays using a single exponential decay function to determine the



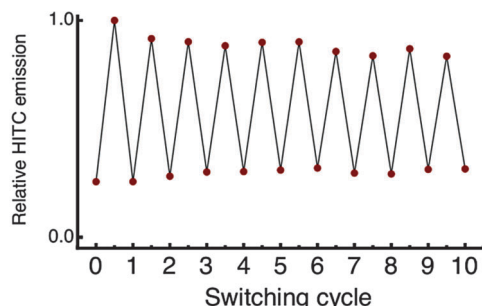


Fig. 4 Relative intensity of the HITC emission following C314 excitation in the C314 + SP/MC + HITC PMMA sample when switching between SP and MC dominant populations using UV and visible light irradiation cycles.

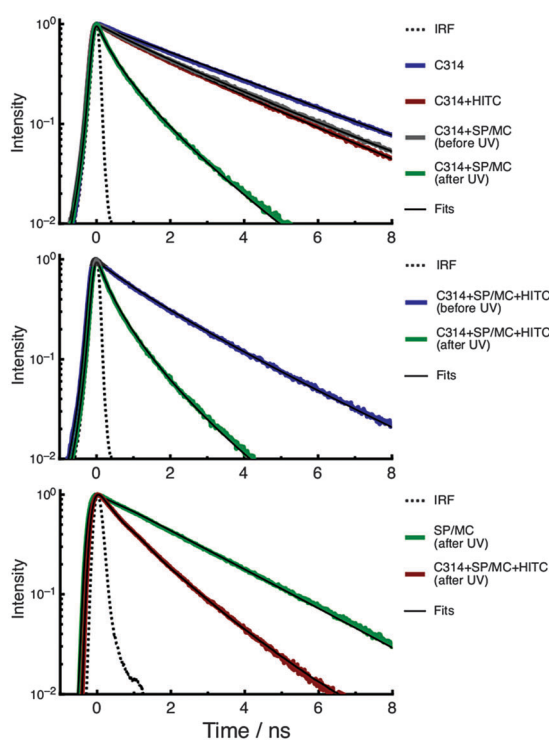


Fig. 5 Fluorescence decay curves of C314 for the C314, C314 + HITC, C314 + SP/MC PMMA samples (top panel). Fluorescence decay curves of C314 for the C314 + SP/MC + HITC PMMA sample (middle panel). Fluorescence decay curves of MC for the SP/MC and C314 + SP/MC + HITC PMMA samples (bottom panel).

excited state lifetime (τ_D). When FRET is present, we fit the decays using a stretched exponential decay function, which provides an experimental estimate of Φ_{FRET} (see ESI†).^{20,21} Parameters derived from the decays are given in Table 1.

The fluorescence decays of C314 were recorded using 435 nm excitation, while monitoring emission at 470 nm. For the C314 sample, the fluorescence decay gives $\tau_D = 3.14$ ns, similar to the value measured in PMMA (3.04 ns) by Felorzbabihi *et al.*¹⁸ For the C314 + HITC sample, the C314 fluorescence decay is slightly faster, with $\Phi_{\text{FRET}} = 0.26$ estimated for the C314 \rightarrow HITC FRET.

Table 1 Photophysical parameters for the dye-doped PMMA samples derived from the fluorescence decay measurements

Sample	τ_D^a (ns)	R_0^b (nm)	Φ_{FRET}^c
C314 fluorescence decay			
C314	3.14		
C314 + HITC		3.8	0.26
C314 + SP/MC		4.1	0.24 ^d /0.85 ^e
C314 + SP/MC + HITC			0.45 ^d /0.88 ^e
MC fluorescence decay			
SP/MC	2.24 ^e		
C314 + SP/MC + HITC		5.5	0.70 ^e

^a Error ± 0.05 ns. ^b Theoretical value. ^c Error ± 0.05 . ^d Before UV irradiation. ^e After UV irradiation.

Before UV irradiation of the C314 + SP/MC sample, the C314 fluorescence decay is slightly faster than that of the pure C314 sample, most likely due to C314 \rightarrow MC FRET involving a small residual population of MC. However, after UV irradiation the C314 fluorescence decay is much faster, due to the increased MC population enhancing C314 \rightarrow MC FRET. From the C314 fluorescence decays we estimate $\Phi_{\text{FRET}} = 0.24$ before UV irradiation and $\Phi_{\text{FRET}} = 0.85$ after UV irradiation for the C314 \rightarrow MC FRET.

The Φ_{FRET} values determined for the C314 + HITC and C314 + SP/MC (before UV irradiation) samples are surprisingly high considering the low concentration of the acceptor species. This is probably due to the occurrence of C314 \rightarrow C314 homo-FRET, allowing the excitation energy to migrate through the sample before undergoing C314 \rightarrow HITC/MC FRET.^{22–24} Indeed, a theoretical $R_0 = 3.2$ nm is calculated for the C314 + C314 pair and we estimate the average spacing between C314 molecules in the PMMA matrix is ~ 5 nm.

For the C314 + SP/MC + HITC sample, the C314 fluorescence decay before UV irradiation is affected by both C314 \rightarrow HITC and C314 \rightarrow MC(residual) FRET, with an estimated $\Phi_{\text{FRET}} = 0.45$: *i.e.*, relaxation back to the C314 ground state still mainly occurs *via* fluorescence and internal conversion. Following UV irradiation, the C314 fluorescence decay becomes much more rapid, due to increased C314 \rightarrow MC FRET, with an estimated $\Phi_{\text{FRET}} = 0.88$.

The fluorescence decays of MC were recorded using 532 nm excitation and monitoring emission between 640–690 nm. For the SP/MC sample after UV irradiation, the MC fluorescence decay gives $\tau_D = 2.24$ ns. This τ_D is significantly longer than that measured for MC in ethanol (0.21 ns),⁹ presumably because the rigid PMMA surroundings restrict the molecule's conformational freedom, decreasing the rate of internal conversion and photoisomerisation. Furthermore, the Φ_R of MC is predicted to increase from 0.02 in ethanol to 0.20 in PMMA (see ESI†).^{9,16} For the C314 + SP/MC + HITC sample after UV irradiation, the MC fluorescence decay is much faster than that of the pure SP/MC sample, due to MC \rightarrow HITC FRET. From the MC fluorescence decays we estimate $\Phi_{\text{FRET}} = 0.70$ for MC \rightarrow HITC FRET after UV irradiation. It is important to recognise that the prolonged τ_D of MC in the PMMA matrix is crucial for the efficiency of the MC \rightarrow HITC step in the FRET cascade.

Overall, the experimental data show that the C314 dye's excitation energy can be appreciably directed towards the HITC dye using a FRET cascade that is controlled by the photochromic SP/MC system.

Research has previously been conducted into the FRET for different combinations of a donor chromophore, acceptor chromophore, and photochromic switch.^{10,13,15} However, in these cases when the switch is in its colourless form, significant donor → acceptor FRET occurs, and when the switch is in its coloured form, it acts as the FRET terminus, either *via* donor → coloured switch FRET and/or donor → acceptor → coloured switch FRET. The photochromic FRET scheme demonstrated here differs from previous constructions in that the overall donor → acceptor energy transfer is enhanced when the switch is converted from colourless to coloured (Fig. 1). An intramolecular version of this FRET cascade scheme was proposed by Jukes *et al.*, yet experimentally the linking SP lost its photochromic ability to convert to MC when bound between two inorganic chromophores.²⁵

A possible application for the photochromic FRET cascade mechanism demonstrated here may involve increasing the spectral contrast of dye-doped polymer nanoparticles that are switchable between two fluorescent states and employed for biological imaging.¹⁴ Another prospective application may lie in developing photonic wires,^{15,26} whereby the donor, switchable bridge, and acceptor are arranged in consecutive nanoscale layers to ensure that energy is transferred in a specific direction.

In conclusion, we have demonstrated that energy transfer from a blue-absorbing dye to a near-IR-absorbing dye embedded in a polymer matrix can be modulated by photoswitching an incorporated SP/MC system. This is the first time the coloured form of a molecular switch has been employed as an intermediate bridge within a FRET cascade.

Acknowledgements

This research was supported under the Australian Research Council's Discovery Project funding scheme (Project DP120100100). V. D. acknowledges an Australian Renewable Energy Agency Postdoctoral Fellowship (6-F004) and support from the University of Melbourne's Early Career Researcher Grant Scheme.

References

- 1 M. Irie, T. Fukaminato, K. Matsuda and S. Kobatake, *Chem. Rev.*, 2014, **114**, 12174–12277.
- 2 R. Klajn, *Chem. Soc. Rev.*, 2014, **43**, 148–184.
- 3 B. L. Feringa, *J. Org. Chem.*, 2007, **72**, 6635–6652.
- 4 F. M. Raymo, *Phys. Chem. Chem. Phys.*, 2013, **15**, 14840–14850.
- 5 J. Andréasson and U. Pischel, *Chem. Soc. Rev.*, 2015, **44**, 1053–1069.
- 6 M. Qin, Y. Huang, F. Li and Y. Song, *J. Mater. Chem. C*, 2015, **3**, 9265–9275.
- 7 S. Straight, P. Liddell, Y. Terazono, T. Moore, A. Moore and D. Gust, *Adv. Funct. Mater.*, 2007, **17**, 777–785.
- 8 M. Bälter, S. Li, J. R. Nilsson, J. Andréasson and U. Pischel, *J. Am. Chem. Soc.*, 2013, **135**, 10230–10233.
- 9 V. Dryza and E. J. Bieske, *J. Phys. Chem. C*, 2015, **119**, 14076–14084.
- 10 J. Walz, K. Ulrich, H. Port, H. Wolf, J. Wonner and F. Effenberger, *Chem. Phys. Lett.*, 1993, **213**, 321–324.
- 11 F. M. Raymo and M. Tomasulo, *Chem. Soc. Rev.*, 2005, **34**, 327–336.
- 12 P. Belser, L. De Cola, F. Hartl, V. Adamo, B. Bozic, Y. Chriqui, V. Iyer, R. Jukes, J. Kühni, M. Querol, S. Roma and N. Salluce, *Adv. Funct. Mater.*, 2006, **16**, 195–208.
- 13 J. H. Hurenkamp, J. J. D. de Jong, W. R. Browne, J. H. van Esch and B. L. Feringa, *Org. Biomol. Chem.*, 2008, **6**, 1268–1277.
- 14 Z. Tian, W. Wu and A. D. Q. Li, *ChemPhysChem*, 2009, **10**, 2577–2591.
- 15 M. Bälter, M. Hammarson, P. Remón, S. Li, N. Gale, T. Brown and J. Andréasson, *J. Am. Chem. Soc.*, 2015, **137**, 2444–2447.
- 16 S. Zhang, Q. Zhang, B. Ye, X. Li, X. Zhang and Y. Deng, *J. Phys. Chem. B*, 2009, **113**, 6012–6019.
- 17 C. S. Santos, A. C. Miller, T. C. S. Pace, K. Morimitsu and C. Bohne, *Langmuir*, 2014, **30**, 11319–11328.
- 18 N. Felorzabihi, P. Froimowicz, J. C. Haley, G. R. Bardajee, B. Li, E. Bovero, F. C. J. M. van Veggel and M. A. Winnik, *J. Phys. Chem. B*, 2009, **113**, 2262–2272.
- 19 Y. Zhao, G. A. Meek, B. G. Levine and R. R. Lunt, *Adv. Opt. Mater.*, 2014, **2**, 606–611.
- 20 J. R. Lakowicz, *Principles of fluorescence spectroscopy*, Springer Science & Business Media, 2007.
- 21 V. Dryza and E. J. Bieske, *J. Phys. Chem. C*, 2014, **118**, 19646–19654.
- 22 R. Métivier, S. Badré, R. Méallet-Renault, P. Yu, R. B. Pansu and K. Nakatani, *J. Phys. Chem. C*, 2009, **113**, 11916–11926.
- 23 L. Gartzia-Rivero, L. Cerdán, J. Bañuelos, E. Enciso, I. L. Arbeloa, Á. Costela and I. García-Moreno, *J. Phys. Chem. C*, 2014, **118**, 13107–13117.
- 24 D. Genovese, E. Rampazzo, S. Bonacchi, M. Montalti, N. Zaccheroni and L. Prodi, *Nanoscale*, 2014, **6**, 3022–3036.
- 25 R. T. F. Jukes, B. Bozic, P. Belser, L. De Cola and F. Hartl, *Inorg. Chem.*, 2009, **48**, 1711–1721.
- 26 E. Graugnard, D. L. Kellis, H. Bui, S. Barnes, W. Kuang, J. Lee, W. L. Hughes, W. B. Knowlton and B. Yurke, *Nano Lett.*, 2012, **12**, 2117–2122.

